In: Bose-Einstein Condensates: Theory, Characteristics... ISBN: 978-1-61728-114-3
Editor: Paige E. Matthews

Chapter 6

MATTER WAVE DARK SOLITONS IN OPTICAL SUPERLATTICES

***Aranya B Bhattacherjee*[1] *and Monika Pietzyk*[2]**
[1]Department of Physics, ARSD College (South Campus),
University of Delhi, India
[2]National Quantum Information Centre of Gdańsk, Sopot, Poland

Abstract

In this work, we study the behaviour of matter-wave band gap spectrum and eigenstates as the periodicity of the optical superlattice is increased. We show that the band gap (between the two lowest bands) which opens up in a doubly periodic superlattice decreases as the periodicity increases further. This is interpreted as a decrease in the Periels-Nabarro barrier which the dark soliton experiences as it goes from one well to the next. For higher periodicity the mobility of the dark soliton is restored.

1. Introduction

When a gas of ultracold atoms is loaded into an optical lattice,its properties are modified strongly [1]. Ultracold bosons trapped in such periodic potentials have been widely used recently as a model system for the study of some fundamental concepts of quantum physics like Josephson effects[2], squeezed states[3], Landau-Zener tunneling and Bloch oscillations[4] and superfluid-Mott insulator transitions[5].

One of the many advantages of a macroscopic quantum periodic system such as a BEC in an optical lattice, is that the effective periodic potential created by a standing light wave can be easily and precisely manipulated by changing the intensities, polarizations, frequencies or geometric arrangement of the interfering laser beams. For example, the depths of the periodic potential wells induced by an optical lattice can be controlled by tuning the intensities of the laser beams. Using superposition of optical lattices with different periods [6], it is now possible to generate more sophisticated periodic potentials characterized by a richer spatial modulation, the so-called optical superlattices. An important and exciting application of optical superlattice is quantum computation [7]. Theoretical interest in optical superlattices started only recently. Examples include work on fractional filling Mott insulator domains [8], dark[9] and gap[10] solitons, the Mott-Peirels transitions[11], non-mean field effects[12] and phase diagrams of BEC in two-colour superlattices[13]. Porter et al.[14] have shown that optical superlattices can manipulate and control solitons in BEC. The analogue of the optical branch in solid-state physics has also been predicted in an optical superlattice [15]. Rousseau et al.[16] have considered the effect of a secondary lattice on a one-dimensional hard core of bosons (strongly correlated regimes). A detailed theoretical study of the Bloch and Bogoliubov spectrum of a BEC in a one-dimensional optical superlattice has been done by Bhattacherjee [17]. In an interesting work [18], we show that due to the secondary lattice, there is a decrease in the superfluid fraction and the number fluctuation. The dynamic structure factor which can be measured by Bragg spectroscopy is also suppressed due to addition of the secondary lattice. The visibility of the interference pattern (the quasi-momentum distribution) of the Mott insulator is found to decrease due to the presence of the secondary lattice. In a very recent experiment [19], it was observed that the center-of-mass motion of a BEC is blocked in a quasi-periodic lattice. This was interpreted as a result of an increase in the effective mass in an superlattice [20]. Most remarkably, periodicity of the optical lattice potential leads to the effective dispersion of the BEC wavepackets being a function of the band structure. In the majority of condensates currently created experimentally, the interatomic interaction is repulsive. This corresponds to an effectively defocusing nonlinearity of the matter-wave which can support dark solitons-localized dips on the condensate density background with a phase gradient across the localized regions. Similar to other types of solitons, they can remain dynamically stable due to the balancing effects of nonlinearity and the (positive) dispersion. Dark solitons have been created experimentally in repulsive condensates by using phase imprinting technique to apply a sharp phase gradient to a condensate cloud in a magnetic trap [21, 22]. In the case of BECs loaded into optical lattices, i.e. with the possibility for dispersion management, dark solitons can be supported in both repulsive (for positive effective dispersion) and attractive condensates (for negative effective dispersion). Moreover, dark lattice solitons are expected to be easier to create experimentally than bright gap solitons as they are not confined to the spectral gaps and a phase imprinting technique can be applied to a nonlinear Bloch-wave background within a spectral band.

The theory of dark solitons has been developed extensively for many types of periodic systems such as discrete atomic chains and waveguide arrays [23, 24, 25, 26, 27]. Applying the concepts of discrete dynamical systems to the physics of the Bose-Einstein condensates in optical lattices, Abdullaev *et al.* [28] studied dark and bright solitons on non-zero backgrounds in a vertical lattice by employing a discrete mean-field model derived in the tight-binding approximation, i.e. considering a single isolated band of the Bloch-wave spectrum. In contrast, Yulin and Skryabin [29] used a single-gap continuous coupled-mode model in order to examine the stability and existence of out-of-gap dark and bright solitons. A more general analysis based on the continuous Gross-Pitaevskii equation with a periodic potential was presented by Alfimov *et al.* [30] who showed that for a repulsive condensate in an optical lattice, dark solitons can exist as stationary localized solutions with nonvanishing asymptotics. Alfimov *et al.* [30] as well as Konotop and Salerno [31] also found numerically stable dark solitons for periodic quasi-one-dimensional BEC systems. The weak spectral instability of the dark solitons in the combined optical lattice and a strong harmonic potential, both in the discrete and continuous mean-field models, has been established in [32].

In this work, we study the behaviour of matter-wave gap spectrum and the eigenstates as the periodicity of the optical superlattice is increased.We study the structure and mobility properties of dark solitons in superlattices by employing the full continuous mean-field model. We show that the band gap (between the two lowest bands) which opens up in a doubly periodic superlattice decreases as the periodicty increases further. This is interpreted as a decrease in the Periels-Nabarro barrier which the dark soliton experiences as it goes from one well to the next. For higher periodicity the mobility of the dark soliton is restored.

2. The Model

We consider an elongated cigar shaped BEC in an optical superlattice. The dynamics of the BEC can be described in the mean-field approximation by the Gross-Pitaevskii (GP) equation for the macroscopic condensate wavefunction $\psi(x,y,z,t)$.

$$i\hbar\frac{\partial\psi(x,y,z,t)}{\partial t} = \left(-\frac{\hbar^2}{2m}\nabla^2 + V_L(x) + V(x,y,z) + g_{3D}|\psi(x,y,z,t)|^2\right)\psi(x,y,z,t), \tag{1}$$

where $V(x,y,z)$ is the time-independent magnetic trapping potential and $g_{3D} = 4\pi\hbar^2$ a_s/m is the two-body interaction with m and a_s as the mass and scattering length of the condensate atoms respectively. We will consider only the case of repulsive interaction. For the cases examined in this paper, we use the parameters set by ^{87}Rb: $m = 1.44\text{x}10^{-25}$ kg and $a_s = 5.7$ nm. We consider an anisotropic parabolic magnetic trapping potential $V(x,r)$ of the form $V(x,r) = \frac{1}{2}m\omega_\perp^2(x^2+\Omega^2r^2) + V_L(x)$, where $r^2 = y^2+z^2$, and $\Omega = \omega_\perp/\omega_x$. The light shifted optical lattice potential of the superlattice is described as

$$V_L = V_0\left(\epsilon\sin^2 k_1x + (1-\epsilon)\sin^2 k_2x\right), \tag{2}$$

where $0 \le \epsilon \le 1$. The superlattice potential can be obtained by creating two separate far-detuned quasi-1D single-periodic lattices using lasers of different wavelengths (Fig.1). If the two lattices are orthogonally polarized, when they are superimposed, the resulting dipole trapping potential is proportional to the sum of their individual intensities. With this interpretation, V_0 is proportional to the total intensity and ε related to the relative intensities of the two standing light waves. The lattice wavevectors are $k_1 = 2\pi/\lambda_1$ and $k_2 = 2\pi/\lambda_2$, and the larger of the two periods is $d = \lambda_1/2$. In this paper we choose $\lambda_1/\lambda_2 = \kappa = 2,4,6$. All length scales are made dimensionless with respect to $a_L = d/\pi$ and energy scales made dimensionless with respect to twice the single photon recoil energy $E_L = \hbar^2/ma_L^2$. Time is made dimensionless with respect to $\tau_L = \hbar/E_L$. The condensate is elongated along the x direction (cigar shaped) and this can be achieved experimentally by making the magnetic trap frequency along the x direction very weak compared to the magnetic trap frequencies along the radial direction. The condensate wavefunction can be separated as $\psi(x,r,t) = \chi(r)\phi(x,t)$, with $\chi(r)$ well described by the ground-state of a two-dimensional radially symmetric quantum harmonic oscillator, with the normalization $\int_{-\infty}^{\infty}|\chi|^2dydz = 1.$. Further since the magnetic trap along the x direction is weak compared to the optical

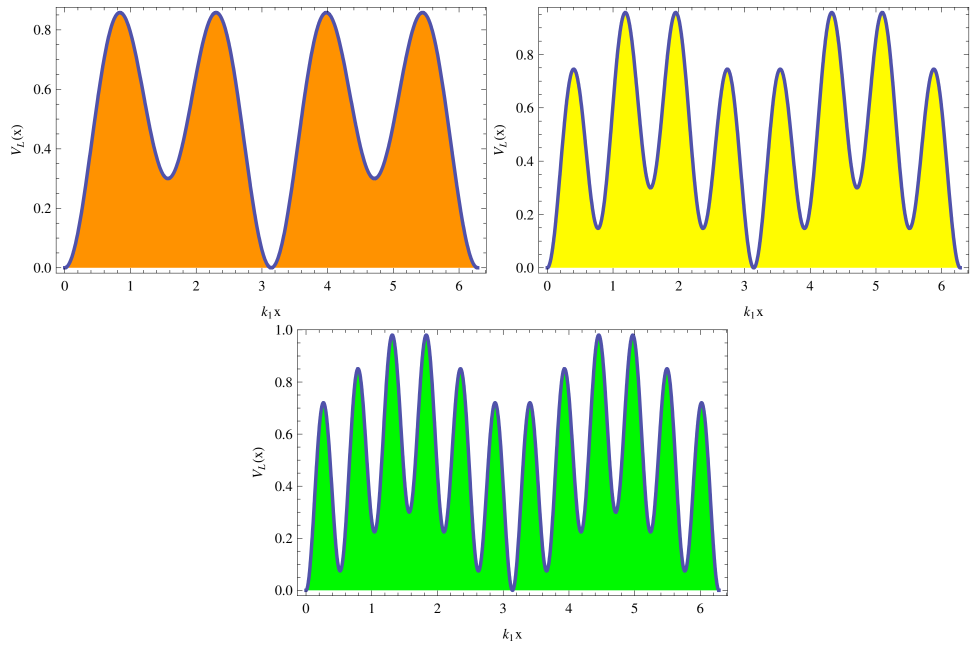

Figure 1. The structure of the superlattice potential described by Eqn.2 for $\epsilon = 0.3$, $V_0 = 1$ and $\kappa = 2$ (top left plot, orange color), $\kappa = 4$(top right plot, yellow color), $\kappa = 6$(bottom plot, green color).

trap, we will ignore it along the x direction. Integrating out the radial coordinates, we obtain the $1D$ GP equation.

$$i\frac{\partial \phi(x,t)}{\partial t} = \left(-\frac{1}{2}\frac{\partial^2}{\partial x^2} + V_L(x) + g_{1D}|\phi(x,t)|^2\right)\phi(x,t), \tag{3}$$

where $g_{1D} = 2(a_s/a_L)(\omega_r/\omega_L)$, ω_r is the radial trap frequency. In the next section we will calculate the matter-wave band-gap sprectrum and the corresponding eigenstates for the superlattices $\kappa = 2, 4, 6$.

3. Matter-wave Band Gap Spectrum and Dark Solitons

Stationary states of Eqn. 3 can be written in the form

$$\phi(x,t) = \Phi(x)exp(-i\mu t), \tag{4}$$

where μ is the corresponding chemical potential. The steady state wavefunction obeys the time-independent GP equation

$$\left(\frac{1}{2}\frac{\partial^2}{\partial x^2} - V_L(x) + \mu - g_{1D}|\Phi(x,t)|^2\right)\Phi(x,t) = 0. \tag{5}$$

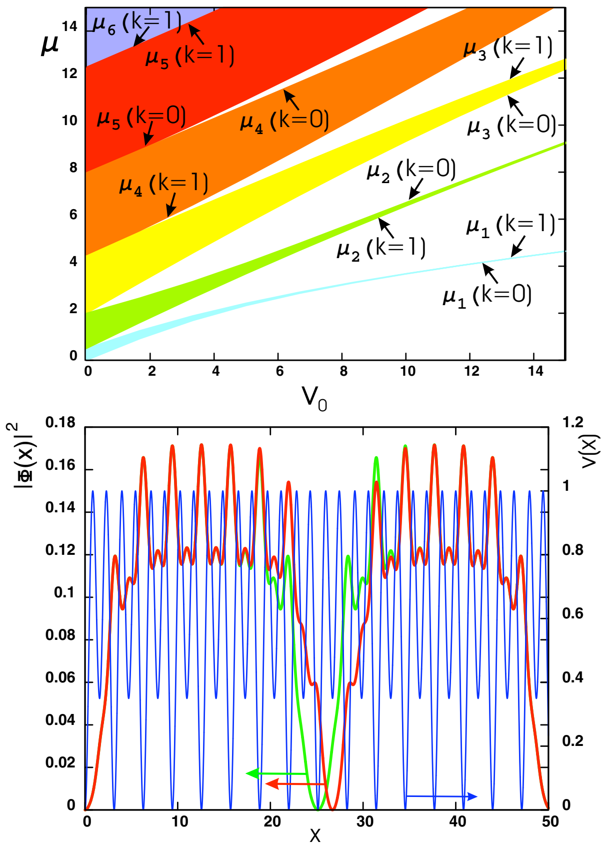

Figure 2. Matter-wave band gap spectrum for the non-interacting condensate in an optical superlattice with $\kappa = 2$ and $\epsilon = 0.3$. The shaded areas are Bloch bands where k is real and the unshaded regions between the bands are the gaps where κ is complex. Also shown is the density profile of dark solitons in the big well and the smallest well.

In order to find the matter-wave band-gap spectrum, we will consider $g_{1D} = 0$ (the case of non-interacting condensate). This condition is true if the number of atoms is small. Eqn. 5 becomes linear in $\Phi(x)$ and the condensate wavefunction can be represented as a superposition of Bloch waves

$$\Phi(x) = a_1\Phi_1(x)e^{ikx} + a_2\Phi_2(x)e^{-ikx}, \tag{6}$$

where $\Phi_{1,2}(x)$ have the periodicity of the lattice potential, $a_{1,2}$ are constants, and k is the Floquet exponent. The matter-wave spectrum in the linear case consists of bands in which k is real. The bands are separated by band-gaps in which k is complex. The solutions at the band edges are exactly periodic stationary Bloch states. Figure 1 presents the band-gap diagram on the plane (μ, V_0) for the Bloch wave solutions of Eqn. 5 in the non-interacting case for a lattice potential described by Eqn.2 for $\kappa = 2$. The spectrum is obtained by solving the matrix eigenvalue problem corresponding to $g_{1D} = 0$ in Eqn.5. Only few lowest bands are shown. Also shown along with the band-gap spectrum is the

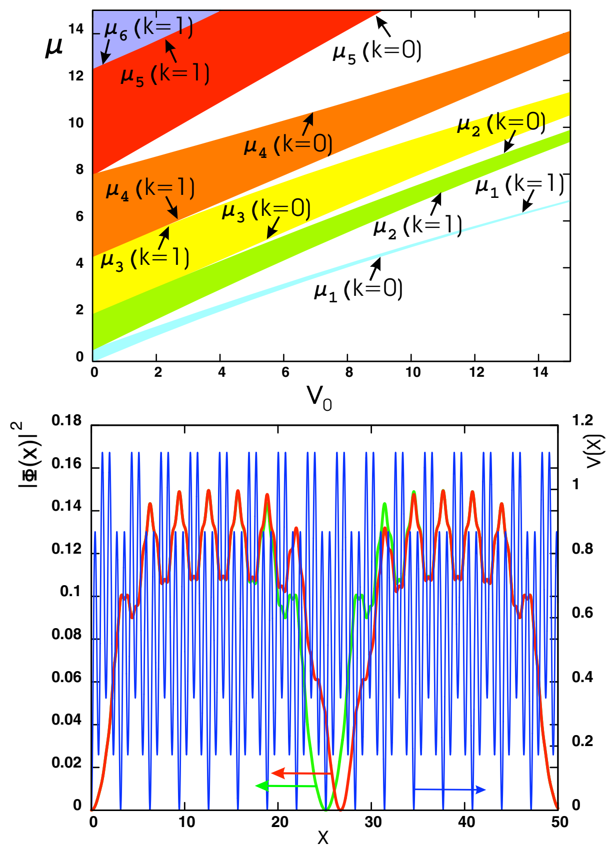

Figure 3. Matter-wave band gap spectrum for the non-interacting condensate in an optical superlattice with $\kappa = 4$ and $\epsilon = 0.3$. Note that the lowest three band-gaps decreases in comparison to the case $\kappa = 2$. The profile of the dark solitons also changes with respect to Fig.1. Noticeable changes in the background is seen.

corresponding density profile of the dark solitons. Note that there are two stable solitons centred at the largest and the smallest well. The density profile consists of the dark soliton and the background. The corresponding potential is also shown for convenience. The background has a spatial structure of a periodic Bloch wave. The matter-wave band-gap spectrum and the corresponding density profiles of the dark solitons for the case $\kappa = 4, 6$ are shown in figures 3 and 4 respectively. Increasing the periodicity of the secondary lattice causes structural changes in the matter-wave band-gap spectrum as well as in the spatial structure of the Bloch states. The gaps which opens up in the $\kappa = 2$ case changes as κ increases. In particular the lowest gap (between $\mu_1(k = 1)$ and $\mu_2(k = 1)$) decreases as κ increases. Correspondingly in the density profile, we find that the width of the dark soliton profile increases as κ increases. The back ground which is a superposition of Bloch waves shows two distinct peaks (one big and one small) for $\kappa = 2$. As κ increases, the smaller peak starts to diminish. This is probably because of the fact for higher periodic superlattice the local periodicity over a few lattice sites is restored and the local influence of

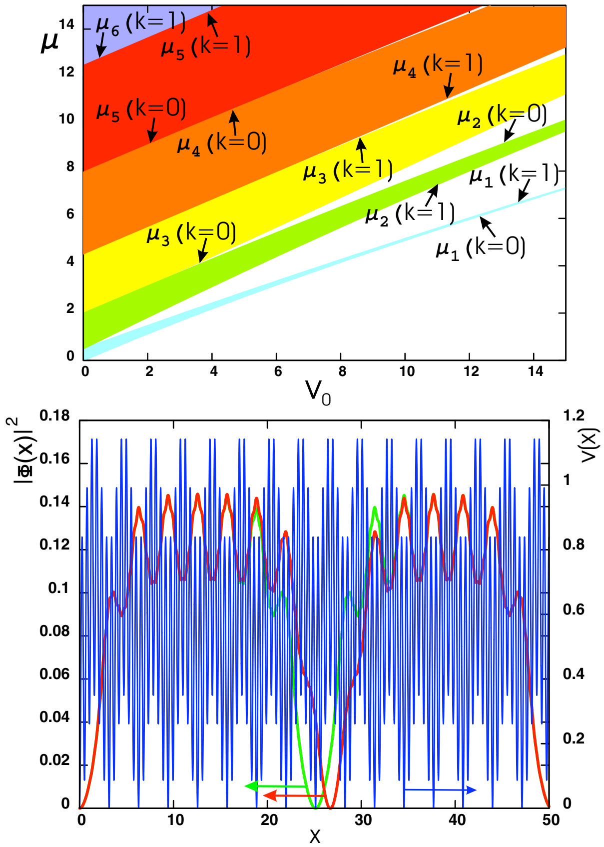

Figure 4. Matter-wave band gap spectrum for the non-interacting condensate in an optical superlattice with $\kappa = 6$ and $\epsilon = 0.3$. The lowest three band-gaps decreases further compared to the case $\kappa = 4$. This is an indication of restoration of mobility of the dark solitons as discussed in the text.

the secondary lattice over a few lattice sites is insignificant. The above observations leads to a speculation that the local mobility of the dark solitons which is reduced for the doubly periodic optical superlattice ($\kappa = 2$) is restored for higher periodic superlattice ($\kappa = 4, 6$). To check this speculation, we calculate the Peierls-Nabarro barrier for different κ's.

4. Peierls-Nabarro Barrier

The energy difference between a soliton centered at a maximum of the periodic potential and one centered at a neighbouring potential minimum corresponds to the height of an effective potential known as the Peierls-Nabarro (PN) potential. The value of the PN potential can be understood as the minimum energy required to move a localized wavepacket by one lattice site and this gives the measure of the mobility of the wavepacket. We calculate the PN potential by calculating at a fixed value of μ the energy difference between dark solitons centered at the biggest minima and the next nearest minima. A fixed value of μ ensures that

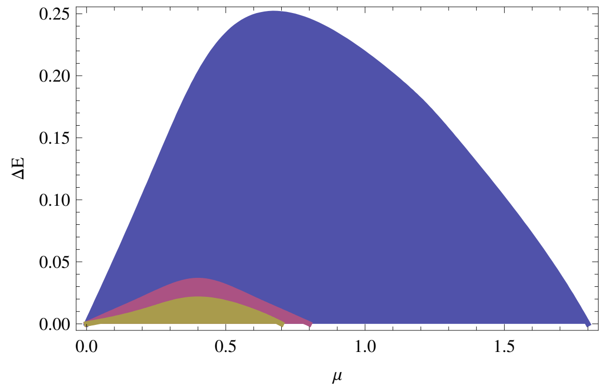

Figure 5. The Peierls-Nabarro (PN) potential versus the chemical potential for $\kappa = 2, 4, 6$. The height of the barrier is decreasing with increasing κ.

the amplitude of the Bloch-wave background is constant, which is the case for a dark soliton moving across the lattice. We analyse the dark solitons originating in the first band. We use the energy functional:

$$E = \int \left\{ \frac{1}{2} \left(\frac{\partial \Phi(x,t)}{\partial x} \right)^2 + V_L(x)\Phi(x,t)^2 + g_{1D}|\Phi(x,t)|^4 \right\} dx. \qquad (7)$$

Strictly speaking this difference is the PN barrier experienced by the dark soliton centered in the neighboring wells. The dark states of the biggest well and the nearest well correspond to the minima and maxima of the PN potential respectively. This means that the biggest minima dark states should be stable, and the next nearest minima states unstable with respect to the variations in their position relative to the lattice. The knowledge of the PN barrier potential height is essential in answering the questions about mobility of the lattice soliton and its ability to interact with other localized states. Fig. 5 shows the PN barrier experienced by a dark soliton in the three different superlattices $\kappa = 2, 4, 6$ as a function of the chemical potential μ. Clearly we see that the PN barrier experienced by a dark soliton in a superlattice decrease as the periodicity increases. This confirms our speculation that the local mobility increases with κ. For moderate values of μ within the first band, the energy difference $\Delta E = E_{next-nearest-well} - E_{biggest-well}$ is positive. Therefore we expect that even in a shallow lattice regime the dark biggest well soliton is effectively pinned by the lattice due to the presence of a large PN barrier. As the periodicity increases, the PN barrier decreases and the lattice is no longer able to pin the soliton. As the periodicity increases, the chemical potential required to release the soliton decreases. The variations in energy difference for different periodicity of the lattice suggests that for a fixed chemical potential, variation in the superlattice parameters controls the mobility and interaction properties of the dark solitons.

5. Conclusions

We have analysed the band-gap structure of the Floquet-Bloch matter waves in optical superlattice structures in the framework of the Gross-Pitaevskii equation. We have shown that band-gaps that initially appear in a double periodic lattice decreases as the periodicity is increased further. This is interpreted as an increase in the soliton mobility and this was confirmed by calculating the Peierls-Nabarro potential barrier which was found to decrease with increasing periodicity of the optical lattice. We have demonstrated that the mobility of the dark solitons can be effectively controlled by changing the periodicity of the optical superlattice.

References

[1] Morsch, O.; Oberthaler, M. *Rev. Mod. Phys* 2006, *78*, 179.

[2] Anderson, B. P.; Kasevich, M. *Science* 1998 *282*, 1686.

[3] Orzel, C. ; Tuchman, A. K.; Fenselau, M. L.; Yasuda, M.; Kasevich, M .A. *Science* 2001 *291* , 2386.

[4] Morsch, O.: Müller, J. M.; Cristiani, M.; Ciampini, D; Arimondo, E. *Phys. Rev. Lett.* 2001 *87*, 140402.

[5] Greiner, M.; Mandel, O.; Esslinger, T.; Hänsch, T. W.; Bloch, I. *Nature* 2002 *415*, 39.

[6] Peil, S et. al. *Phys. Rev. A.* 2003 *67* 051603(R).

[7] Sebby-Strabley. J et. al. *Phys. Rev A* 2006 *73*, 033605.

[8] Buonsante. P; Vezzani, A. *Phys. Rev. A* 2004 *70*, 033608.

[9] Louis, P. J. Y.; Ostrovskaya, E. A; Kivshar, Y. S.; *J. Opt. B* 2004 *6*, S309.

[10] Louis, P. J. Y.; Ostrovskaya, E. A; Kivshar, Y. S.; *Phys. Rev. A* 2005 *71*, 023612.

[11] Dmitrieva L. A.; Kuperin, Y. A.; Cond-mat/0311468.

[12] Rey, A. M.; Hu, B. L.; Calzetta, E.; Roura, A.; Clark, C. W.; *Phys. Rev. A* 2004 *69*, 033610 .

[13] Roth, R.; Burnett, K,; *Phys. Rev. A* 2003 *68*, 023604.

[14] Porter, M. A.; Kevrekidis, P. G.; Carretero-Gonzalez, R.; Frantzeskakis, D. J.; *Phys. Letts. A* 2006 *352*, 210.

[15] Huang, Chou-Chun.; Wu, Wen-Chin. *Phys. Rev. A* 2005 *72*, 065601.

[16] Rousseau, V. G.; Arovas, D. P.; Rigol, M.; Hébert, F.; Batrouni, G. G.; Scalettar, R. T.; *Phys. Rev. B* 2006 *73*, 174516.

[17] Bhattacherjee, A. *J. Phys.B. At. Mol. Opt. Phys.* 2007 *40*, 143.

[18] Bhattacherjee, A. *Eur. Phys. J. D* 2008 *46*, 499.

[19] Lye, J. E. et. al. *Phys. Rev. A* 2007 *75*, 061603.

[20] Bhattacherjee, A.; Pietzyk, M. *Cent. Eur. J. Phys.* 2008 *6*, 26.

[21] Burger, S. et. al. *Phys. Rev. Lett.* 1999 *83*, 5198.

[22] Denschlag, J. et. al. *Science* 2000 *287*, 97.

[23] Peyrard, M.; Kruskal, M. D.; *Physica D* 1984 *14* 88.

[24] Kevrekidis, P. G; Weinstein, M. I.; *Physica D* 2000 *142* 113.

[25] Ablowitz, M. J.; Musslimani, Z. H.; *Phys. Rev. E* 2003 *67* 025601.

[26] Sukhorukov, A. A.; Kivshar, Y. S.; *Phys. Rev. E* 2002 *65* 036609.

[27] Feng, J.; Kneubühl, F. K. *IEEE J. Quantum Electron.* 1993 *29* 590.

[28] Abdullaev, F. Kh.; Baizakov, B.B.; Darmanyan, S. A.; Konotop, V. V.; Salerno, M *Phys. Rev. A* 2001 *64* 043606.

[29] Yulin, A. V.; Skryabin, D. V. *Phys. Rev. A* 2003 *67* 023611.

[30] Alfimov, G. L.; Konotop, V. V.; Salerno, M. *Europhys. Lett.* 2002 *58* 7.

[31] Konotop V. V.; Salerno. M. *Phys. Rev. A* 2002 *65* 021602.

[32] Kevrekidis, P. G.; Carretero-Gonzalez, R.; Theocharis, G.; Frantzeskakis, D. J.; Malomed, B. A. *Phys. Rev. A* 2003 *68*, 035602.